# REALISTIC MODELING OF MEBT FOR THE NEW LANSCE RFQ INJECTOR

S.S. Kurennoy, LANL, Los Alamos, NM 87545, USA

## Abstract

The new RFQ-based proton injector at LANSCE requires a specialized medium-energy beam transfer (MEBT) after the RFQ at 750 keV due to a following long (~3 m) existing common transfer line that also transports H$^-$ beams to the DTL entrance. The horizontal space for MEBT elements is limited because two beam lines merge at 18-degree angle. The MEBT includes two compact quarter-wave RF bunchers and four short quadrupoles with steerers, all within the length of about 1 m. The beam size in the MEBT is large, comparable to the beam-pipe aperture, hence non-linear 3D fields at large radii and field-overlap effects become important. With CST Studio codes, we calculate buncher RF fields and quadrupole and steerer magnetic fields, and use them for particle-in-cell beam dynamics modeling of MEBT with realistic beam distributions from the RFQ. Our results indicate a significant emittance growth in MEBT not predicted by the standard beam dynamics codes. Its origin is traced mainly to the quadrupole edge fields; the buncher RF fields also contribute noticeably. Proposed design modifications improve the MEBT performance.

## INTRODUCTION

A modern front end for the LANSCE linac is under development: the aging Cockcroft-Walton based injectors will be replaced by modern RFQ-based ones [1]. Now two lines, one for H$^+$ (proton) and the other for H$^-$ ions, produce 750-keV beams that merge into a common transport, which goes to the entrance of the first DTL tank. The proton injector will be upgraded first, but the existing common transport line for different beam species creates significant constrains for the injector line design. The first challenge is a very long distance from the proton RFQ exit to the DTL entrance, almost 4 m. Second, because the two beam lines merge at 18-degree angle, the horizontal space for proton-line elements is limited by the existing hardware near the merging area. Therefore, a specialized medium-energy beam transfer (MEBT) after the new proton RFQ at 750 keV was developed [2] with envelope codes, and the beam dynamics in MEBT was modeled using Parmila [3]. The MEBT shapes the RFQ output beam to transfer it through the long existing common transport to the DTL with minimal losses. The MEBT includes four electromagnetic (EM) quadrupole magnets and two buncher cavities [2], all within about 0.9 m along the beam line, followed by a 0.5-m long drift to the merging point of the common transport line, which continues for ~2.6 m to the DTL entrance. The beam pipe in the injector line has inner diameter (ID) 1.875" (aperture radius $a \approx 2.381$ cm) and outer diameter 2"; the pipe wall thickness is 1/16" ($\approx 0.159$ cm).

The proton beam size in the MEBT is large, comparable to the beam-pipe aperture; therefore, non-linear 3D field effects at large radii become important, both in bunchers and quadrupoles. We calculated buncher RF fields and quadrupole and steerer magnetic fields with CST Studio codes [4], and applied them in particle-in-cell (PIC) beam dynamics modeling of MEBT [5]. The beam transverse emittances increase after MEBT significantly more than predicted by design [2]. Here we study the effects of MEBT element modifications and the beam transport to DTL using PIC simulations with CST Particle Studio (PS).

## MEBT AND TRANSPORT TO DTL

The main MEBT elements are two compact quarter-wave (QW, $\lambda/4$) 201.25-MHz RF cavity bunchers and four short EM quadrupole magnets with additional windings for beam steering. Both elements have a small footprint on the beamline, shorter than 8 cm. The QW buncher is a coaxial resonator with two gaps separated by distance $\beta\lambda/2 = 2.98$ cm for $\beta = 0.04$ [5, 6]. The bunchers (B) and quadrupoles (Q) are arranged in the MEBT in the following order: $Q_1$, $B_1$, $Q_2$, $Q_3$, $Q_4$, and $B_2$. The buncher and quadrupole EM parameters and fields were calculated in CST MicroWave and EM Studios, see details in [6]. The maximal effective voltage of QW buncher in the design [2] is $V_{eff} = 25$ kV (12.5 kV per gap). The quad effective length is 7.6 cm with gradients $G$ from 7.1 to 10.8 T/m.

The beam envelopes in the MEBT and transport to DTL corresponding to the design [2] are shown in Fig. 1. The MEBT includes elements 1-12 in Fig. 1. The proton and H$^-$ beams merge in the bending dipole (elements 14-16), then pass through the main buncher (20) and a long drift (21-36) with 4 tuning quadrupoles to the DTL entrance. The main buncher (MB) is a single-gap reentrant 201.25-MHz cavity with a narrow aperture of 1-cm radius.
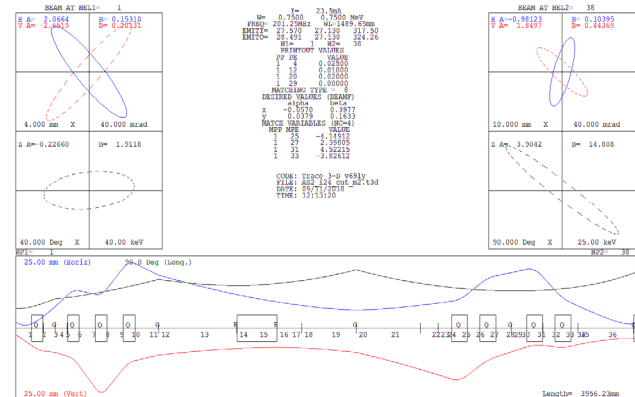


Figure 1: Trace 3D beam envelopes in the proton RFQ MEBT and common transport line to DTL.

# BEAM DYNAMICS

## Initial Beam Distributions

For initial beam distributions in PIC modeling of MEBT and following beam line we use two realistic distributions for the proton beam at the RFQ exit from previous macro-particle simulations, the same as in [5, 6]. In both cases, a 24-mA current beam was simulated with 10K macro-particles at the RFQ entrance. The first output distribution (A) is from ParmteqM runs (L. Rybarcyk), converted into PS input format. The second (B) is from our PS simulations of the RFQ [7] that used MWS-calculated 3D RFQ fields. Some parameters of these initial beam distributions are summarized in Table 1, cf. [5, 6] for more details.

Table 1: Initial Beam Distribution Parameters

| Parameter, units | A | B |
|---|---|---|
| Proton beam current, mA | 23.5 | 22.6 |
| Number of macro-particles $N$ | 9788 | 9397 |
| Average particle energy, keV | 750 | 754 |
| Norm. rms emittance $\varepsilon_x$, $\pi$ μm | 0.22 | 0.25 |
| Norm. rms emittance $\varepsilon_y$, $\pi$ μm | 0.22 | 0.25 |
| Rms longit. emittance $\varepsilon_z$, $\pi$ μm | 0.28 | 0.35 |

## MEBT PIC Simulation Results

The MEBT models use scaled CST-calculated buncher RF fields and quad magnet fields. The effective voltages are 25 kV in $B_1$ and 18 kV in $B_2$ [2], with RF phases properly set for bunching as the bunch center arrives at the cavity center [6]: 180° in $B_1$ and 152° in $B_2$ for input A. For input B, the beam energy is corrected (-4 keV) in $B_1$, so the RF phase is 167° in $B_1$ and 152° in $B_2$.

The beam dynamics has been modeled with the CST PS PIC solver by running the initial beam through the MEBT fields. The particle parameters are recorded using 2D plane particle monitors in the exit plane, at 15 cm from the B2 center. The beam steering was added as necessary using CST-calculated steerer fields to minimize the beam-center displacements along the MEBT [6]. We considered various MEBT configurations in [5, 6], e.g., substituting CST-computed quad fields (EM) by ideal quadrupole fields (HE), turning bunchers on and off, etc. Some important simulation results from [5, 6] are listed in Table 2.

Table 2: Parameter Changes vs. MEBT Configuration

| # | D | Q | $N/N_0$ | $\varepsilon_x/\varepsilon_{x0}$ | $\varepsilon_y/\varepsilon_{y0}$ | $\varepsilon_z/\varepsilon_{z0}$ |
|---|---|---|---|---|---|---|
| 1 | A | EM | 0.979 | 3.14 | 1.77 | 1.36 |
| 2 | A | HE | 0.991 | 1.68 | 1.14 | 1.18 |
| 3 | B | EM | 0.968 | 3.08 | 2.32 | 1.37 |
| 4 | B | HE | 0.979 | 1.92 | 1.24 | 1.26 |

The notations in Table 2 are D for initial distribution, Q for quads; the ratios in the last four columns are for final / initial values. The beam transverse emittances increase significantly: the horizontal $\varepsilon_x$ by a factor of ~3, the vertical $\varepsilon_y$ by a factor of <2, for the realistic MEBT with EM quads (#1). For the PS input (B), the emittance behavior is similar (#3). Such large emittance increases are unexpected and much higher than ~30% predicted by design [2] for transverse emittances. On the other hand, the longitudinal emittance increases by ~35% for both distributions, mainly in the second buncher, $B_2$, while the design [2] predicts much larger increase, by 128%.

We explored possible reasons for such a large transverse emittance growth and how it can be mitigated. Some can be attributed to the differences between Trace/Parmila and CST models: (i) Parmila uses ideal hard-edge quadrupole fields, and (ii) the bunchers in Parmila are modeled as zero-length single gaps, with longitudinal and transverse kicks to the passing particles that depend on the particle radial position. With ParmteqM input (A), we compared various MEBT configurations: realistic quad fields (EM) vs. ideal ones (HE), turning bunchers on and off, etc. [5, 6]. With HE-quad fields the emittance growth is noticeably smaller, cf. #2 vs. #1 and #4 vs. #3 in Table 2. It was found that steerer effects are small. QW bunchers work slightly better than 1-gap ones for the same wide apertures [6]. The buncher fields mostly affect the horizontal emittance, increasing it by a factor of 1.5 on top of the space charge increase. With bunchers off, the EM quad fields increase the horizontal emittance by a factor of ~1.75 above the space charge. Finally, the combined effect of the buncher RF fields and realistic quadrupole magnetic fields on the transverse emittances was approximately multiplicative.

Some MEBT elements modifications were necessary to mitigate the emittance growth. First, quadrupole design modifications were introduced to reduce the field non-linearities at large radii and edge fields: increasing the quad aperture and/or length; replacing EM (some or all) with permanent-magnet quadrupoles (PMQ); or adjusting pole-tip shapes [6, 5]. Two possible options are shown in Fig. 2.
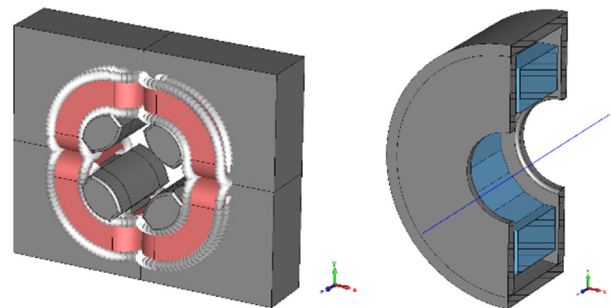


Figure 2: Quad modifications: EM quad with extended core (left) and 16-segment PMQ with outer shield (right).

The EM quadrupole with extended inner core (Fig. 2, left) increases the region of good field without increasing the quad footprint. The PMQ with an outer shield for clamping edge fields (Fig. 2, right) allows small adjustments of $GL$ by changing the shield dimensions.

Obviously, with PMQs additional steerers are still needed. Some PIC simulation results for modified MEBT with B input were given in [6, 5]. Additional results for a few MEBT configurations are presented in Table 3, for comparison with Table 2.

Table 3: Parameter Changes vs. MEBT Configuration

| # | D | Q | $N/N_0$ | $\varepsilon_x/\varepsilon_{x0}$ | $\varepsilon_y/\varepsilon_{y0}$ | $\varepsilon_z/\varepsilon_{z0}$ |
|---|---|---|---|---|---|---|
| 5 | A | PMQ | 0.988 | 2.64 | 2.18 | 1.21 |
| 6 | A | PMQL | 0.988 | 2.41 | 1.73 | 1.21 |
| 7 | A | E/PM | 0.988 | 2.64 | 1.77 | 1.25 |

The cases in Table 3 are: #5 – short PMQs; #6 – longer PMQs with shielding; #7 – combined EM ($Q_{1,4}$) and long shielded PM ($Q_{2,3}$) quadrupoles. The last configuration allows steering with EM quads. Compared to Table 2 (#1), one can see some improvements, though the emittance growth is still quite large.

### PIC Simulations of Transport to DTL and DTL

To evaluate how the beam after MEBT is transported to and captured in the DTL, we followed it along the transport line and in the first tank (T1) of DTL. Two distributions after MEBT were chosen for these PIC simulations – cases #2 and #3 in Table 2, as the best (the closest to design [2]) and the worst (though more realistic) case. The magnetic field of the merging dipole and RF fields of the main buncher (MB) were calculated with CST. The MB voltage was set at 20 kV [2]. We used hard-edge magnet fields for the large-aperture (3"-diameter) quadrupoles in the drift from MB to DTL. Finally, beam dynamics in the DTL T1 was studied using a CST model developed earlier [8].

As one can expect, the results for two cases are quite different. In case #2, the beam losses in the transport are relatively small (1.8% in MB, 4.6% in the drift). The emittances at the DTL entrance are $\varepsilon_{x,y,z} = 0.29, 0.25, 0.45$ $\pi$ $\mu$m, close to the design values [2] and those used as input in [8]. Comparing with values in Tables 1-2, we see that an exchange between transverse and longitudinal emittances occurs. However, the beam fraction captured into a bunch and accelerated to 5.4 MeV in T1 is only 86.4%, compared to 95% for a similar beam after RFQ [8]. This difference is due to a beam mismatch at the DTL entrance. For case #3, the transport beam losses are significant: 22% is scraped by the narrow aperture of MB, and 5.7% more is lost in the drift. Clearly, the MEBT should be tuned differently in this case to provide a waist at MB. The beam emittances at the DTL entrance are $\varepsilon_{x,y,z} = 0.50, 0.41, 0.68$ $\pi$ $\mu$m, and the capture in T1 is only 82.2%, again due to an even larger beam mismatch at the linac entrance. We conclude that the beam transmission to and its capture in DTL are very sensitive to the MEBT setup. The MEBT should be tuned for a particular beam distribution coming out of the RFQ, taking into account the realistic 3D fields of MEBT elements, to optimize the transmission through the common transport line and match the beam to the DTL.

## CONCLUSION

We explored beam dynamics in the MEBT for the new RFQ-based proton injector at LANSCE and the following beam transport line to the DTL with CST Particle Studio particle-in-cell (PIC) 3D simulations to take into account effects of the large beam size and field overlaps. The CST-calculated fields of quarter-wave RF buncher cavities and of quadrupole magnets with steerers in MEBT [5, 6] were used. For the transport line PIC simulations we calculated RF fields of the main buncher and the magnetic field of the merging dipole. We found that the transverse emittances increase significantly more than was predicted in the original MEBT design [2], which was based on the standard approach using envelope codes and Parmila simulations. One the other hand, the longitudinal emittance growth is lower than predicted [2]. The differences are due to a very large beam size in MEBT, which is required to further transfer the beam through a long transfer line to DTL. 3D effects and field overlaps of adjacent elements become essential but cannot be taken into account by traditional beam dynamics codes. From this viewpoint, it is one more example where simulations with standard codes are insufficient to predict beam dynamics correctly.

The emittance growth is caused mainly by the magnetic fields of short EM quadrupoles. The buncher RF fields also contribute. We considered some modifications of the MEBT quads and demonstrated their positive effects. However, further MEBT optimization is still required. Our results show that the beam transmission through the common transport and its capture in the DTL are rather sensitive to the MEBT setup, which should be adjusted with account of 3D effects.

## ACKNOWLEDGMENT

## REFERENCES

[1] R.W. Garnett *et al.*, "Status of the LANSCE front-end upgrade," in *Proc. NA-PAC13*, Pasadena, CA, 2013, p. 327.

[2] C.M. Fortgang *et al.*, "A specialized MEBT design for the LANSCE H$^+$ RFQ upgrade project," in *Proc. NA-PAC13*, Pasadena, CA, USA, Sep.-Oct. 2013, TUPSM17, p. 670.

[3] Los Alamos Accelerator Code Group, laacg.lanl.gov

[4] CST Studio Suite, CST, www.cst.com

[5] S.S. Kurennoy, "3D beam dynamics modeling of MEBT for the new LANSCE RFQ injector," in *Proc. IPAC18*, Vancouver, BC, Canada, Apr.-May. 2018.
doi:10.18429/JACoW-IPAC2018-TUPAL035

[6] S.S. Kurennoy, Tech notes AOT-AE: 17-009, 18-005; "Beam dynamics modeling of the proton RFQ MEBT with CST PS," LA-UR-18-23434, Los Alamos, 2018.

[7] S.S. Kurennoy, "3D effects in RFQ accelerators," in *Proc. Linac14*, Geneva, Switzerland, 2014, THPP097, p. 1077.

[8] S.S. Kurennoy, "Beam dynamics modeling of drift-tube linacs with CST Particle Studio," in *Proc. IPAC16*, Busan, Korea, p. 689.
DOI:10.18429/JACoW-IPAC2016-MOPOR042